光学学报

高信噪比随机光电振荡器

李阳，余游，徐恩明，张祖兴*

南京邮电大学先进光子技术实验室，江苏 南京 210023

摘要　提出和研究了一种高信噪比(SNR)随机光电振荡器(ROEO)。该 ROEO 由随机光纤激光器与光电振荡器两部分组成，得益于随机光纤激光器中瑞利散射(RS)提供的随机分布反馈，实现了宽带随机微波信号的产生。通过在随机光纤激光器中加入另一个波分复用器(WDM)，去除残余的拉曼泵浦光，提高了随机微波信号的信噪比。控制信号光的偏振态，抑制了随机腔中的受激布里渊散射(SBS)效应。实验中，获得了带宽为 DC～30 GHz(DC 代表直流 0 Hz，表达的含义是从 0 Hz 到 30 GHz)的随机微波信号。在 DC～10 GHz 范围内的信噪比约为 40 dB，并且腔内的受激布里渊散射与随机微波信号的功率差达到约 19.64 dB。高信噪比宽带随机微波信号在随机比特生成、雷达、安全通信等领域有重要的应用前景。

关键词　微波光子学；随机光电振荡器；瑞利散射；波分复用器；高信噪比

中图分类号　O436　　　**文献标志码**　A　　　　　　　　　　　　**DOI:** 10.3788/AOS230782

1　引　　言

近年来，光电振荡器(OEO)由于具有高频、大带宽、抗电磁干扰等显著优点得到了快速发展，广泛用来产生超低相位噪声的微波光子信号，主要应用于通信[1]、雷达[2]、测量[3]等重要领域。在过去的几十年中，已经发展出双环光电振荡器[4-6]、耦合光电振荡器[7-9]、注入锁定光电振荡器[10-12]和宇称-时间对称(PT symmetry)光电振荡器[13-15]等。1997 年，Yao 等[16]采用双环光电振荡器降低相位噪声，随后又提出了耦合性光电振荡器，通过使用光学环路和光电环路耦合组成的 OEO，极大地缩减光纤腔长度，增大自由光谱区(FSR)，以减小模式竞争，同时还具有高 Q 值。2005 年，Zhou 等[17]设计了注入锁定双环光电振荡器，该振荡器通过使用长光纤环路主振荡器将注入锁定到短环路信号模式从振荡器中。与当前最先进的在 10 GHz 频率下工作的多环路 OEO 相比，该振荡器在降低相位噪声和减少杂散方面有了显著的改进，初步相位噪声测量结果表明杂散电平降低了大约 140 dB。Liu 等[18]在 2018 年研究了 PT 对称系统在光电振荡器中的应用，PT 对称系统可以产生具有高光谱纯度的单频正弦信号。在具有两个相互耦合的有源振荡腔的 OEO 中，通过精确操纵两个振荡腔中增益和损耗之间的相互作用，对 PT 对称性进行了理论分析和实验观察。

这些不同结构的光电振荡器可以产生高频微波信号和复杂的微波信号，比如利用外加调制产生的啁啾微波信号[19]、锁相微波信号[20]、混沌信号[21]等。但上述光电振荡器都依赖自身的光纤腔长，产生的振荡频率单一且频率调谐受限。2020 年，中国科学院半导体研究所李明教授课题组[22]将光纤中后向瑞利散射与光电振荡结合起来，构建了宽带随机光电振荡器，利用后向瑞利散射，在开放腔中获得了超宽带(DC～40 GHz)随机微波信号。所产生的信号具有随机特性，其振荡频率不受谐振腔固定长度的限制。随机信号在许多领域具有潜力，如随机比特生成[23]、雷达系统、电子干扰和对抗。但因为有源放大器件，开环噪声引入了很大的基底噪声，随机信号功率仅仅高于噪声功率 20 dB。关于随机微波信号信噪比改善的方案还没有报道。

本文提出了一种能产生高信噪比随机微波信号的 ROEO。ROEO 由随机光纤激光器和光电振荡环路组成，通过在随机腔中引入波分复用器(WDM)，去除剩余的拉曼泵浦功率，改善随机微波信号的信噪比(SNR)。调节偏振控制器(PC)，控制信号光的偏振态，抑制了色散补偿光纤(DCF)中的受激布里渊散射效应。可调谐激光器的功率为 12.6 dBm、拉曼泵浦功率为 28.2 dBm 时，生成了 DC～30 GHz 宽带随机微波信号。在 DC～10 GHz 带宽下，随机信号功率比噪声功率高约 40 dB，并且功率平坦。高信噪比随机微波信号在噪声雷达系统、目标检测和电磁干扰等方面具有广阔的应用前景。

2 基本原理

2.1 原理分析

所提高信噪比 ROEO 原理如图 1 所示，实线和虚线分别表示光路信号和电信号。可调谐激光器（TLS）输出功率为 7.4 dBm～12.6 dBm 的窄线宽激光，其作为信号光，随后信号光进入 PC。当拉曼泵浦光和信号光同偏振时，拉曼增益有最大值；当拉曼泵浦光和信号光正交偏振时，拉曼增益有最小值。实验中，利用 PC 来抑制光纤中的受激布里渊散射效应。
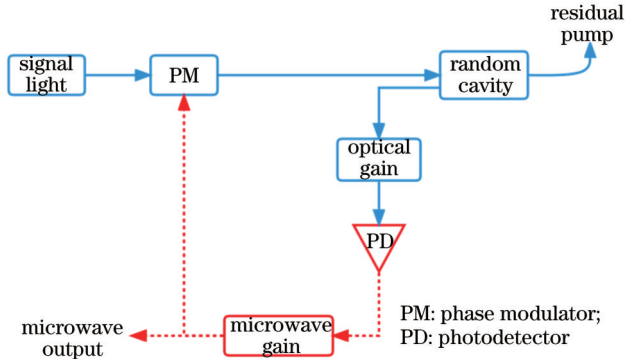

图 1 高信噪比随机光电振荡器示意图

Fig. 1 Schematic of random optoelectronic oscillator with high signal-to-noise ratio

调节偏振态后的信号光被电放大器（EA）驱动的相位调制器（PM）调制，调制后的信号光可以表示为

$$E_1 = E_0 \exp(\mathrm{j}\omega_0 t)\exp[\mathrm{j}\gamma\cos(\omega_m t)], \quad (1)$$

式中：ω_0 是泵浦光频率；ω_m 是调制频率；γ 是调制指数。调制后的光信号经过隔离器从光环形器（Cir）的 1 端口进入，2 端口输出，进入随机腔中。由波长为 1455 nm/1550 nm 的 WDM1 将拉曼泵浦光与波长为 1555 nm 的信号光送入 DCF。为了将多余拉曼光排出腔外，增加了 WDM2，同时为了避免光纤尾端的菲涅耳散射的影响，在随机腔的尾端增加了光隔离器。DCF 末端混合输出的 1455 nm 拉曼泵浦光和 1555 nm 信号光进入 WDM2 的合波端，残余拉曼泵浦光从 WDM2 的 1455 端口排除，信号光从 1550 端口进入 ISO2 排除。瑞利散射发生在 DCF 的不同位置，随机光电振荡器的环路长度可以表示为

$$L_i = L_0 + Z_i, \quad (2)$$

式中：L_0 是减去 OEO 随机光纤腔长的回路长度；Z_i 是随机光纤腔中发生瑞利散射的不同位置距离 DCF 输入端的长度。随机腔中后向瑞利散射场表达为

$$\Delta\varepsilon_b(t, z_i) = M(z_i)\varepsilon_s(t - 2z_i/v)\mathrm{e}^{-\alpha z_i}\mathrm{e}^{-\mathrm{j}2\beta z_i}\Delta\rho(z_i), (3)$$

式中：$\Delta\rho(z_i)$ 为反向散射系数；$M(z_i)$ 表示瑞利散射场的偏振状态；α、β 及 v 分别为衰减系数、传播常数及群速度。瑞利散射光从光环形器 2 端口进入，3 端口输出到光放大器，经光电探测器（PD）转换为光电流，光电流经电放大器增益后反馈到相位调制器，形成光电振荡回路。传统的固定腔长光电振荡器的振荡频率与腔长有关：

$$f_{osc} = mc/nL, \quad (4)$$

$$\Delta f = c/nL = 1/\tau, \quad (5)$$

式（4）表示传统单频 OEO 振荡频率集合，m 表示纵模数量，L 是 OEO 环路长度；式（5）表示模式间隔。ROEO 产生的宽带随机微波信号相当于不同腔长的单频 OEO 的输出总和。随机分布位置的瑞利后向散射导致信号频率的连续变化和信号功率的随机波动，而不是单个或离散的一组固定值。不同频率的波总是能找到相应的腔长来满足相干相加条件。
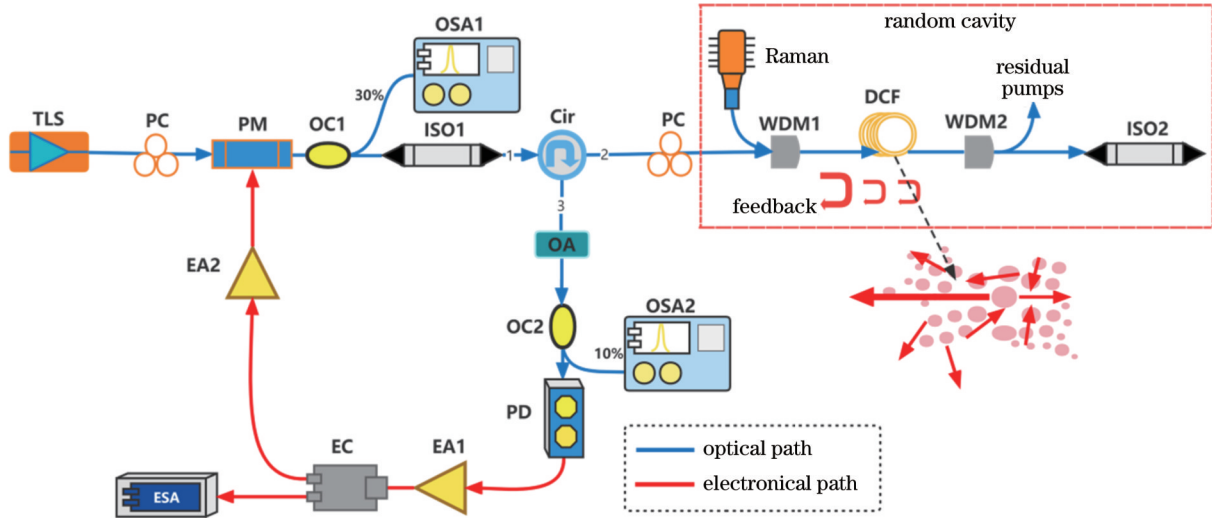
$$\varepsilon_b(t) = \sum_{n=1}^N \varepsilon_b(t, n\Delta l), \quad (6)$$

式（6）显示 ROEO 环路内后向散射场的叠加腔内的功率呈现出随机波动，ROEO 输出的随机微波信号振幅表示出明显的随机波动。ROEO 环路内光学总增益与电总增益之和大于环路内的损耗时，ROEO 达到起振条件。

2.2 实验结果

搭建的实验装置如图 2 所示。随机信号的生成过程可以具体描述为：TLS 输出波长为 1555 nm、功率为 12.6 dBm 的信号光，信号光经 PC 后传输到相位调制器（MPZ-LN-10，Ixblue 公司）。调制器的半波电压 $V_\pi = 4.1$ V，V_0 是驱动电压，相位调制器的调制指数 $\gamma = \pi V_0/V_\pi$。采用了超低插损 1.7 dB 的相位调制器，不需要额外控制调制器的工作点，改善了强度调制器工作点漂移的缺点。PM 输出的光信号由 1:99 的耦合器（OC）分光。1% 端口的输出用来观测信号光和闭环后光谱的变化，由分辨率为 0.02 nm 的光纤光谱仪（AQ-6370D）测量。99% 端口的信号光经过光隔离器进入光环形器的 1 端口，这里隔离器主要用来阻止随机腔中的后向散射光穿透光环形器来干扰信号光。信号光从光环形器的 2 端口与波长为 1455 nm 的拉曼泵浦光通过 WDM1 合光，在长度为 7.2 km 的 DCF 中激发后向瑞利散射，光纤中随机分布的瑞利散射光构成随机分布反馈。瑞利散射可以发生在 DCF 的任意位置，所以 OEO 的环路长度不确定，符合条件的频率都可以在 OEO 中振荡。

在 DCF 后加上一个 WDM2，滤除残余拉曼泵浦光功率。后向传播的瑞利散射光从光环形器的 2 端口到 3 端口，光放大器将微弱的后向散射光功率放大 10 dB。从 OC2 的 10% 端口可以测量放大后的光谱和进入 PD（DC～18 GHz）的光功率，90% 功率光耦合进环路内。PD 将光信号转换为电信号，电信号经增益为 20 dB 的 EA1（DC～15 GHz）传输到 5:5 的电分束器。50% 功率的微波信号由频谱分析仪（RMS FSV30）测量，另外 50% 微波信号经 27 dB 的 EA2（IXblue DR-AN-10-HO，DC～10 GHz）二次放大反馈到 PM 中，构成完整的 ROEO。当环路中的增益大于损耗，满足条

TLS: tunable laser; PC: polarization controller; OC: optical coupler; ISO: optical isolator; OSA: optical spectrum analyzer; Cir: optical circulator;
Raman: Raman laser; WDM: wavelength division multiplexer; DCF: dispersion compensated fiber; OA: optical amplifier; EA: electric amplifier;
EC: electric coupler; ESA: electrical spectrum analyzer

图 2   高信噪比随机光电振荡器的实验装置

Fig. 2   Experimental device of random optoelectronic oscillator with high signal-to-noise ratio

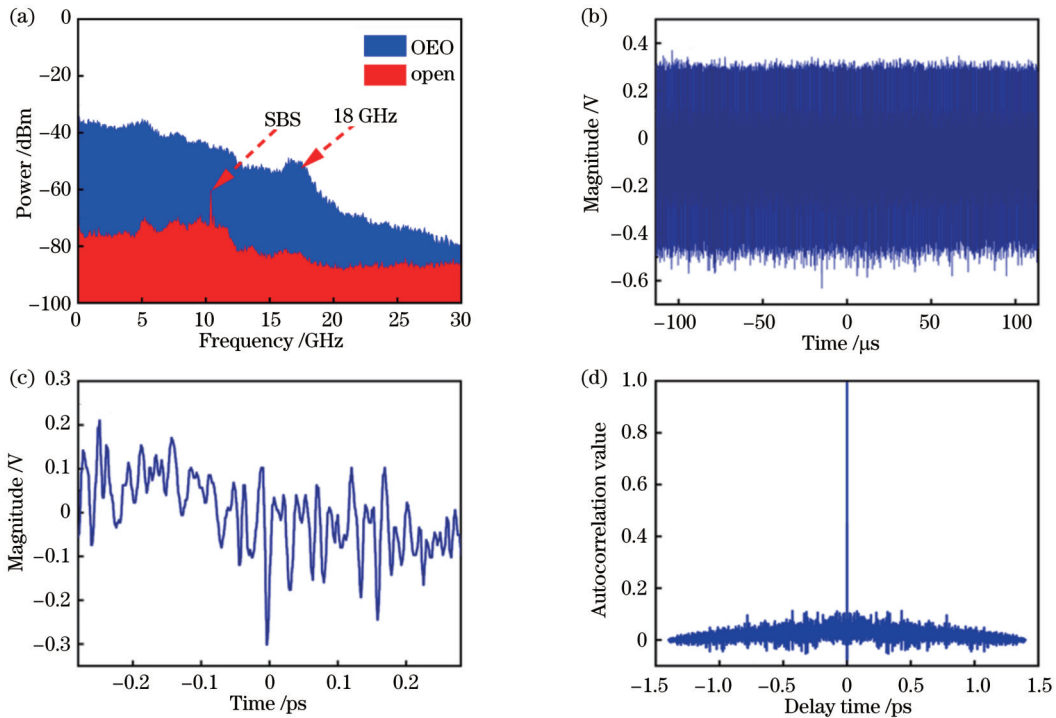件的不同频率的微波同时发生振荡。通过调整拉曼泵浦功率至 28.2 dBm，可以实现图 3(a)所示的带宽为 DC～30 GHz 的随机信号，开环噪声抑制可以达到约 40 dB。

图 3   随机光电振荡器产生的随机微波信号。(a)0～30 GHz随机信号，包括振荡的 OEO 信号和开环基底噪声；(b)采样率为 4 GSa/s 的示波器随机信号的 200 μs 时域谱；(c)时间宽度为 0.56 ps 的随机信号的时域波形；(d)时域波形的自相关函数仿真

Fig. 3   Random microwave signal generated by a random optoelectronic oscillator. (a) 0-30 GHz random signal, including oscillating OEO signal and open-loop substrate noise; (b) 200 μs time-domain spectrum of oscilloscope random signal with sampling rate of 4 GSa/s; (c) time-domain waveform of random signal with time width of 0.56 ps; (d) simulation of autocorrelation function of time-domain waveform

由于所使用 PD 的带宽是 DC～18 GHz，18～30 GHz 的频谱功率是迅速衰减的。DC～18 GHz 的频谱出现不平坦是因为 EA1 的放大带宽为 15 GHz，EA2 的放大带宽为 10 GHz。频谱分析仪（RMS FSV30）的

分辨率带宽（RBW）为 500 kHz，视频带宽（VBW）为 500 kHz，ESA 的截止带宽为 30 GHz。拉曼增益与偏振相关，通过 PC 调节信号光的偏振状态，衰减拉曼增益，抑制 DCF 中的受激布里渊散射（SBS）效应。与文献[22]相比，斯托克斯光信号与随机微波信号的功率对比抑制效果提升约 15 dB。

3　分析与讨论

为了对产生的随机信号进行性能评估，使用采样率为 4 GSa/s 的实时示波器测量了 200 μs 左右的随机信号，如图 3(b)所示。图 3(c)是截取 0.56 ps 的微波信号，信号的振幅和频率都无周期性地随机变化。对时域信号的自相关函数进行计算，结果如图 3(d)所示，近似为 delta 函数，自相关函数在延迟时间为 0 时具有最大值，当延迟时间处于其他时刻，自相关函数的函数值近似为 0。证明了生成的信号是随机无序的，类似白噪声，信号具有不可预测性。图 3(d)中其他时刻自相关函数的值不完全趋近于 0，是因为示波器的采

样率有限，造成采样点数不足，采用高分辨率示波器可以避免这个问题。

OC1 的 1% 端口与 OC2 的 10% 端口分别由 OSA1 和 OSA2 测量，结果如图 4(a)和图 4(b)所示。虚线光谱表示开环条件下没有反馈回路时测量的光谱，实线光谱是 ROEO 振荡时测量的光谱。构成 OEO 反馈回路后，腔中符合振荡条件的频率起振。图 4(a)ROEO 光谱展宽是反馈到 PM 的带宽为数十 GHz 的随机微波信号导致的，形成了双边带（DSB）调制，1555 nm 载波两边出现了光谱功率上升的现象。光谱不平坦是因为探测器的响应带宽和电放大器增益带宽有限，更高频的随机微波信号得不到响应和放大。图 4(b)ROEO 光谱是经随机腔压缩后的光谱，随机光纤激光器会对输入光进行线宽压缩，相比于图 4(a)光谱展宽，减小了许多。图 4(b)的光谱没有受到探测器和电放大器的影响，1555 nm 附近的光谱较平坦。OSA2 测量的图 4(b)虚线光谱的小突起是斯托克斯光，表明信号光经过 DCF 后产生了受激布里渊散射，这与 3(a)的频谱图相对应。
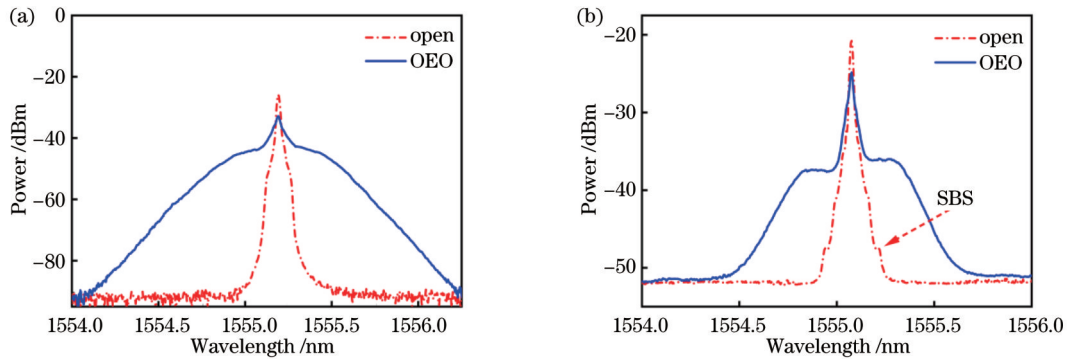

图 4　OEO 光谱与开环光谱。(a) OSA1 测量的光谱；(b) OSA2 测量的光谱

Fig. 4　OEO spectrum and open-loop spectrum. (a) Spectrum measured by OSA1; (b) spectrum measured by OSA2

图 5(a)为 DC～10 GHz 的射频信号和开环噪声，功率差异显著，大约为 40 dB，显示了所提系统优异的噪声抑制能力，这是因为 WDM2 剥离出过剩的拉曼泵浦功率，减弱了基底噪声。相比文献[22]中的 20

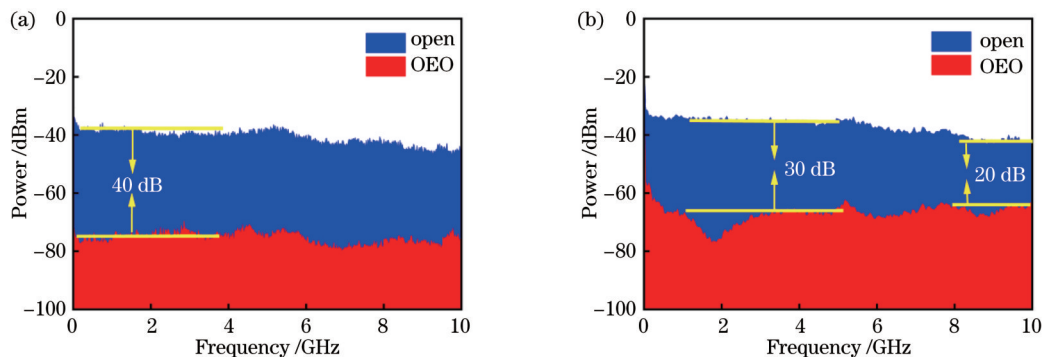dB 功率差值，本 OEO 系统的增益更突出，并且 DC～10 GHz 的射频功率比较平坦，如果两级电放大器拥有更宽的放大带宽，可以实现带宽更大的平坦随机微波信号。去掉 WDM2 后结果如图 5(b)所示，开环基

图 5　WDM2 对随机微波信号的信噪比的影响。(a)采用 WDM2，随机微波信号信噪比达 40 dB；(b)无 WDM2，随机微波信号信噪比在 20 dB～30 dB 范围内

Fig. 5　Effect of WDM2 on SNR of random microwave signals. (a) Using WDM2, SNR of random microwave signal reaches 40 dB; (b) without WDM2, SNR of the random microwave signal is in the range of 20 dB to 30 dB

底噪声增大，DC～10 GHz 的 OEO 功率与噪声功率在 20 dB 到 30 dB 之间，当反馈回路闭合构成 OEO，OSA1 处观测到的功率增大。与文献［22］相比，本文采用了插入损耗更低的 PM，OEO 微波功率更有效地反馈到腔内，OEO 振荡功率与开环功率相差更大。

图 6(a)为开环条件下 WDM2 对 OSA2 测量的光谱的影响，图 6(b)是 OEO 条件下 WDM2 对 OSA2 测量的光谱的影响。OEO 条件下，控制 PC 调节信号光

的偏振态与 WDM2 滤除拉曼泵浦功率配合，消除了斯托克斯光，结果如图 6(b)所示。OEO 环路中无 WDM2 时，调节 PC 后斯托克斯光仍旧存在。开环条件下，相比有 WDM2 的情况，无 WDM2 情况下的功率高 12.15 dB；OEO 条件下，相比有 WDM2 的情况，无 WDM2 情况下功率高 9.05 dB。这与图 7 中 OEO 的随机微波信号功率结果一致。加入 WDM2 会剥离部分 OEO 腔内功率，表现为光谱功率和频谱功率的降低。
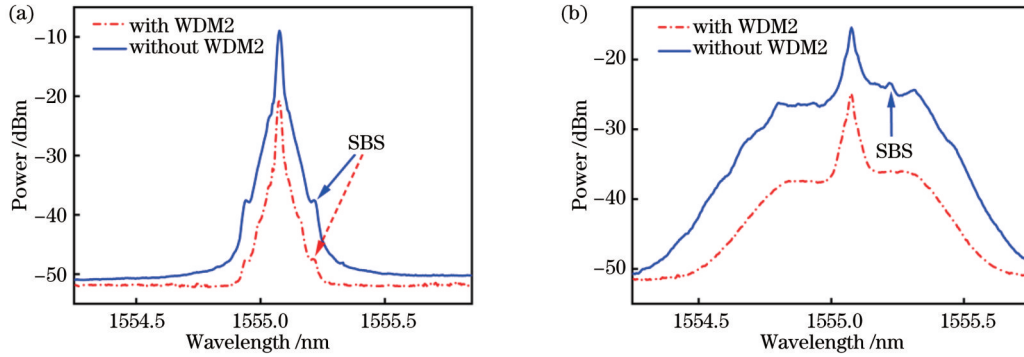

图 6 WDM2 对光谱的影响。(a)开环条件；(b) OEO 条件

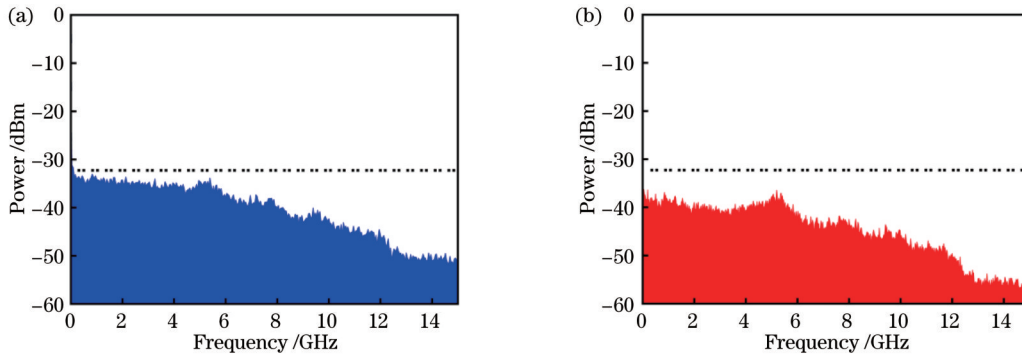Fig. 6 Effect of WDM2 on optical spectrum. (a) Open-loop condition; (b) OEO condition

图 7 WDM2 对信号功率的影响。(a)不采用 WDM2，OEO 的随机微波信号；(b)采用 WDM2，OEO 的随机微波信号

Fig. 7 Effect of WDM2 on signal power. (a) Random microwave signal of OEO without WDM2; (b) random microwave signal of OEO with WDM2

图 8 为含有 WDM2 时不同拉曼增益条件下的随

图 8 不同拉曼泵浦功率对随机微波信号功率的影响

Fig. 8 Effect of different Raman pumping power on the power of random microwave signal

机微波信号，并且与 ESA 基底噪声作对比。在低拉曼增益条件下，随机光电振荡器的后向瑞利散射偏弱，耦合进 ROEO 的光功率较低。随着拉曼泵浦的增加，瑞利散射逐渐增强，ROEO 随机微波功率稳步提高，可以看出拉曼增益对 ROEO 输出功率起关键作用，说明输出功率主要得益于腔内的增益大小。在随机信号功率最高时，信噪比依旧达约 40 dB。
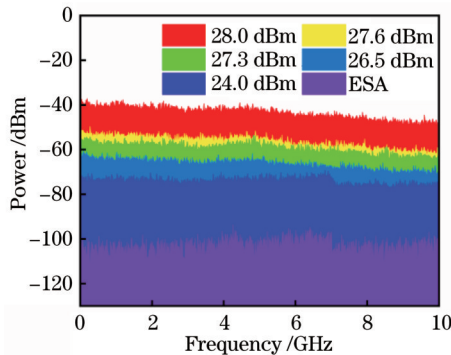
4 结 论

提出了一种高信噪比的 ROEO，产生的随机微波信号在 DC～10 GHz 平坦度较好并且噪声抑制达到 40 dB。利用 WDM2 剥离出随机腔中过剩的拉曼泵浦光，提升 ROEO 的信噪比。通过 PC 控制信号光的偏振态来减小拉曼增益，从而抑制 OEO 环路中的受激布

里渊散射效应。ROEO 的开放腔突破了传统 OEO 产生单频微波信号的限制，生成的宽带随机微波信号在噪声雷达系统、电磁干扰、保密通信、随机编码领域有广阔的应用潜力。窄带滤波器可以产生窄带随机信号，应用于信道加密。

参 考 文 献

[1] Prasad R. Overview of wireless personal communications: microwave perspectives[J]. IEEE Communications Magazine, 1997, 35(4): 104-108.

[2] Peng Z Y, Li C Z. Portable microwave radar systems for short-range localization and life tracking: a review[J]. Sensors, 2019, 19(5): 1136-1155.

[3] Plant W J, Keller W C, Hayes K. Measurement of river surface currents with coherent microwave systems[J]. IEEE Transactions on Geoscience and Remote Sensing, 2005, 43(6): 1242-1257.

[4] Jiang Y, Yu J L, Wang Y T, et al. An optical domain combined dual-loop optoelectronic oscillator[J]. IEEE Photonics Technology Letters, 2007, 19(11): 807-809.

[5] Jia S, Yu J L, Wang J, et al. A novel optoelectronic oscillator based on wavelength multiplexing[J]. IEEE Photonics Technology Letters, 2015, 27(2): 213-216.

[6] 江阳, 于晋龙, 王耀天, 等. 一种新型双环路光电振荡器[J]. 光学学报, 2007, 27(5): 919-922.
Jiang Y, Yu J L, Wang Y T, et al. A novel scheme of dual-loop optoelectronic oscillator[J]. Acta Optica Sinica, 2007, 27(5): 919-922.

[7] Dahan D, Shumakher E, Eisenstein G. Self-starting ultralow-jitter pulse source based on coupled optoelectronic oscillators with an intracavity fiber parametric amplifier[J]. Optics Letters, 2005, 30(13): 1623-1625.

[8] Williams C, Davila-Rodriguez J, Mandridis D, et al. Noise characterization of an injection-locked COEO with long-term stabilization[J]. Journal of Lightwave Technology, 2011, 29(19): 2906-2912.

[9] 刘亮亮, 李晓琼, 戴键, 等. 基于非保偏光纤环腔的启钥式耦合光电振荡器[J]. 中国激光, 2022, 49(18): 1815001.
Liu J L, Li X Q, Dai J, et al. On-key coupled photoelectric oscillator based on non-polarization maintaining fiber ring cavity[J]. Chinese Journal of Lasers, 2022, 49(18): 1815001.

[10] Okusaga O, Adles E J, Levy E C, et al. Spurious mode reduction in dual injection-locked optoelectronic oscillators[J]. Optics Express, 2011, 19(7): 5839-5854.

[11] Lee K H, Kim J Y, Choi W Y. Injection-locked hybrid optoelectronic oscillators for single-mode oscillation[J]. IEEE Photonics Technology Letters, 2008, 20(19): 1645-1647.

[12] 李元栋, 蒲涛, 顾因, 等. 基于直调光信号注入半导体激光器构建宽调谐可集成光电振荡器[J]. 光学学报, 2022, 42(13): 1323003.
Li Y D, Pu T, Gu Y, et al. Construction of wide tuning integrable photoelectric oscillator based on directly modulated light signal injection into semiconductor laser[J]. Acta Optica Sinica, 2022, 42(13): 1323003.

[13] Zhang J J, Yao J P. Parity-time-symmetric optoelectronic oscillator[J]. Science Advances, 2018, 4(6): eaar6782.

[14] Fan Z Q, Zhang W F, Qiu Q, et al. Hybrid frequency-tunable parity-time symmetric optoelectronic oscillator[J]. Journal of Lightwave Technology, 2020, 38(8): 2127-2133.

[15] Teng C H, Zou X H, Li P X, et al. Fine tunable PT-symmetric optoelectronic oscillator based on laser wavelength tuning[J]. IEEE Photonics Technology Letters, 2020, 32(1): 47-50.

[16] Yao X S, Maleki L. Dual microwave and optical oscillator[J]. Optics Letters, 1997, 22(24): 1867-1869.

[17] Zhou W M, Blasche G. Injection-locked dual opto-electronic oscillator with ultra-low phase noise and ultra-low spurious level[J]. IEEE Transactions on Microwave Theory and Techniques, 2005, 53(3): 929-933.

[18] Liu Y Z, Hao T F, Li W, et al. Observation of parity-time symmetry in microwave photonics[J]. Light: Science & Applications, 2018, 7: 38-47.

[19] Hao T F, Cen Q Z, Dai Y T, et al. Breaking the limitation of mode building time in an optoelectronic oscillator[J]. Nature Communications, 2018, 9: 1839.

[20] Hao T F, Cen Q Z, Guan S H, et al. Optoelectronic parametric oscillator[J]. Light: Science & Applications, 2020, 9: 102-112.

[21] Romeira B, Kong F Q, Figueiredo J M L, et al. High-speed spiking and bursting oscillations in a long-delayed broadband optoelectronic oscillator[J]. Journal of Lightwave Technology, 2015, 33(2): 503-510.

[22] Ge Z T, Hao T F, Capmany J, et al. Broadband random optoelectronic oscillator[J]. Nature Communications, 2020, 11: 5724.

[23] Ge Z T, Xiao Y, Hao T F, et al. Tb/s fast random bit generation based on a broadband random optoelectronic oscillator[J]. IEEE Photonics Technology Letters, 2021, 33(22): 1223-1226.

Random Optoelectronic Oscillator with High Signal-to-Noise Ratio

Li Yang, Yu You, Xu Enming, Zhang Zuxing*

Advanced Photonic Technology Lab, Nanjing University of Posts and Telecommunications, Nanjing 210023, Jiangsu, China

Abstract

Objective　In recent years, optoelectronic oscillators (OEOs) have undergone rapid development due to their remarkable advantages such as high frequency, large bandwidth, and magnetic interference immunity. They are widely used to generate microwave photonic signals with ultralow phase noise level, which are mainly used in important fields such as communications, radar systems, and measurements. In the past decades, double-loop, coupled, injection-locked, and

cosymmetric-time symmetry (parity-time symmetry) OEOs have been developed. These different structures of OEOs can be used to generate high-frequency microwave signals as well as complex microwave signals, such as chirped microwave signals via applied modulation, phase-locked microwave signals, and chaotic signals. However, the abovementioned OEOs rely on their own fiber cavity lengths to produce a single oscillation frequency with a limited frequency tuning range. In 2020, Prof. Ming Li's group at the Institute of Semiconductors, Chinese Academy of Sciences, proposed to combine backward Rayleigh scattering (RS) in an optical fiber with optoelectronic oscillation to realize a broadband random OEO (ROEO), and an ultra-broadband (DC‒40 GHz) random microwave signal is obtained in an open cavity through backward RS. The generated signal possesses random characteristics, and its oscillation frequency was not limited by the fixed length of the resonant cavity. Random signals have potential in many applications such as random bit generation, radar systems, and electronic jamming and countermeasures. However, their open-loop noise results in a large substrate noise because of the active amplifier devices, and the random signal power is only 20 dB greater than the noise power. Schemes for improvement of the signal-to-noise ratio (SNR) of random microwave signals have not been reported. In this study, we propose an ROEO for the generation of high-SNR random microwave signals. The ROEO consists of a random fiber laser and an optoelectronic oscillation loop, which improves the SNR of random microwave signals by introducing a wavelength division multiplexer (WDM) in the random cavity and eliminating the remaining Raman pump power. The regulated polarization controller (PC) controls the polarization state of the signal light to suppress the stimulated Brillouin scattering (SBS) effect in the dispersion-compensating fiber (DCF).

Methods　　The ROEO consists of two devices: a random fiber laser and an OEO. Broadband random microwave signals are generated by the ROEO through random distribution feedback provided by RS in the random fiber laser. The SNR of the random microwave signal generated by the ROEO is improved by adding another WDM (WDM2) to the random fiber laser to eliminate the residual Raman pump light from the random cavity. The polarization state of the signal light is controlled by the PC to reduce the Raman gain and thus suppress the SBS effect in the OEO loop. The signal light from port 2 of the optical circulator (OC) is combined with 1455-nm Raman pump light via WDM1 and excited in the DCF at 7.2 km for achieving RS to produce a random distributed feedback. RS can occur at any position in the DCF; therefore, the loop length of the OEO is not determined, and all eligible frequencies can oscillate in the OEO. WDM2 is added to the system following the DCF to filter out residual Raman-pumped optical power. The backscattered Rayleigh light propagates from port 2 to port 3 of the OC, and the optical amplifier amplifies the weak, backscattered optical signal by 10 dB. 10% port of OC2 allows for the measurement of the amplified spectrum and the optical power in the photodetector (PD) (DC‒18 GHz), with 90% power coupling into the loop. The PD converts the optical signal into an electrical one, which is fed through electronic amplifier 1 (EA1) (DC‒15 GHz). The microwave signal with 50% power is analyzed using a spectrum analyzer, and the remaining 50% microwave signal is fed back to a phase modulator (PM) through secondary amplification by EA2 with 27-dB gain, which constitutes the complete ROEO. When the loop gain exceeds the loop loss, the microwaves with different frequencies oscillate simultaneously.

Results and Discussions　　In Fig. 3(a), DC‒30 GHz bandwidth is shown for a random signal for which the open-loop noise rejection may reach ∼40 dB. The power of the spectrum for 18‒30 GHz frequencies rapidly decays because the bandwidth of the PD used is DC‒18 GHz. The spectrum obtained for DC‒18 GHz has uneven distribution because the amplification bandwidth of EA1 and EA2 is 15 and 10 GHz, respectively. The resolution bandwidth of the spectrum analyzer (RMS FSV30) is 500 kHz, the video bandwidth is 500 kHz, and the cutoff bandwidth of ESA is 30 GHz. The Raman gain is dependent on polarization, and the SBS effect in the DCF is suppressed by the adjustment of the polarization state of the signal light by the PC to attenuate the Raman gain. Compared with systems presented in the literature, the power contrast suppression of the Stokes optical signal and the random microwave signal is improved by ∼15 dB by the present system. The RF signal and open-loop noise plots for DC‒10 GHz, shown in Fig. 5(a), which exhibit a significant power difference of ∼40 dB, show the excellent noise rejection of the present system, which is due to WDM2 that eliminates the excess Raman pump power and attenuates the substrate noise. Compared with the 20-dB power difference achieved in previous studies, the gain of the present OEO system is more prominent and the RF power is more uniform for DC‒10 GHz. In addition, the system can generate random microwave signals with a large bandwidth if the two-stage EA has a wider amplification bandwidth. Upon removing WDM2, as shown in Fig. 5(b), the open-loop substrate noise level increases and the OEO power at DC‒10 GHz is between 20 dB and 30 dB from the noise power, when the feedback loop is closed to form OEO, the power observed at OSA1 increases. Compared with the literature, our study uses a PM with a lower insertion loss (1.7 dB); the OEO microwave power is more effectively fed back into the cavity, and the difference between the OEO oscillation power and the open-loop power is higher.

Conclusions　　This study demonstrates a high-SNR ROEO that generates random microwave signals with good flatness when considering DC‒10 GHz and a noise rejection of 40 dB. The SNR of the ROEO is enhanced by stripping the excess

Raman-pumped light from the random cavity using WDM2. The polarization state of the signal light is controlled using a PC to reduce the Raman gain and thus suppress the SBS effect in the OEO loop. The open cavity of the ROEO eliminates the limitation of conventional OEOs of generating single-frequency microwave signals，and the generated broadband random microwave signals exhibit considerable application potential in noisy radar systems，electromagnetic interference，secure communications，and random coding. Narrowband random signals can be generated using narrowband filters for channel encryption applications.

Key words microwave photonics; random optoelectronic oscillator; Rayleigh scattering; wavelength division multiplexer; high signal-to-noise ratio